

Simulation of Color of Port Wine Stain Skin and Its Dependence on Skin Variables

Wim Verkruysse, PhD, Gerald W. Lucassen, PhD, and
Martin J.C. van Gemert, PhD*

Laser Center, Academic Medical Center, University of Amsterdam, 1150 AZ Amsterdam
Z.O., The Netherlands

Background and Objective: The understanding of why Port Wine Stain (PWS) skin is redder and darker as compared to normal skin has so far been based on qualitative analysis. This study aims at quantitatively analyzing the influence of skin anatomy variables on perceived skin color.

Study Design/Materials and Methods: Reflectance spectra for visible light from normal and Port Wine Stain skin have been calculated using a Monte Carlo algorithm applied to a multi-layered skin model. Skin parameters that were varied are pigmentation, dermal scattering, dermal blood concentration, blood oxygenation, vessel diameter, and vessel depth. The CIE 1976 color system was used to interpret the resulting spectra as colors.

Results: A reduced dermal blood content results in a less red and lighter color. Distribution of a constant volume of blood in smaller vessels results in a redder and darker color. Skin with higher dermal scattering was calculated to be yellower and lighter and skin with increased epidermal pigmentation results in a yellower and darker color.

Conclusions: Redness of PWS skin depends on both the concentration of dermal blood as well as on how it is distributed. *Lasers Surg. Med.* 25:131–139, 1999. © 1999 Wiley-Liss, Inc.

Key words: Monte Carlo; blood; light scattering; reflectance spectrum

INTRODUCTION

Treatment of Port Wine Stains (PWS) by laser is based on selective photothermolysis. Ectatic vessels, containing hemoglobin, are the target absorbers that are irreversibly damaged due to heat produced by light absorption [1]. Studies to determine ideal laser parameters have shown that knowledge of the PWS characteristics, such as dermal blood content and vessel diameter, is of vital importance to optimizing laser treatment [2–6].

One of the possible methods that may allow determination of PWS characteristics is reflectance spectrophotometry. Spectra of normal and PWS skin have been shown in several studies [7–9]. Measured reflectance spectra (450 nm to 800 nm) were compared to simulated spectra calculated with a diffusion model of light propaga-

tion [10]. In the present study we show simulated reflectance spectra using a Monte Carlo method of photon propagation. Since Monte Carlo algorithms are based upon transport theory this enables us to calculate reflectance in the blue region below 450 nm where the diffusion approximation

Contract grant sponsor: Dutch Technology Foundation; Contract grant number: AGN33.2964.

Wim Verkruysse's current address is: Beckman Laser Institute and Medical Clinic, Irvine, California.

Gerald W. Lucassen's current address is: Philips Research Laboratories, Eindhoven, The Netherlands.

*Correspondence to: Martin J. C. van Gemert, Laser Center, Academic Medical Center, University of Amsterdam, Meibergdreef 9, 1105 AZ Amsterdam Z.O., The Netherlands.
E-mail: m.j.vangemert@amc.uva.nl

Accepted 16 March 1999

may be less accurate. This is important since the visible spectrum ranges from about 400 nm to 700 nm and, therefore, reflectance levels below 450 nm contribute significantly to the perceived color of skin.

Since reflectance spectra are difficult to interpret in terms of perceived color we have used the L^*, a^*, b^* (CIE 1976) system to represent reflectance spectra as a point in a three-dimensional homogeneous color space. This enables interpretation of different PWS anatomies as different colors and to calculate color differences between normal and PWS skin. An advantage of using this color system is that color values can be easily measured in a clinical situation with a color meter [11].

Our first objective is to investigate the influence of dermal blood concentration, PWS vessel diameter, epidermal pigmentation, dermal scattering, and blood oxygenation, on the simulated perceived color using a two-layered skin model. Our second objective is to calculate resulting color changes after simulated laser treatments of PWS anatomy.

MATERIALS AND METHODS

Monte Carlo Computations and PWS Anatomy

We used a Monte Carlo program (adapted from Keijzer et al. [12]) to calculate the fraction of diffusely back scattered light from various multi-layered skin models (Fig. 1). Total skin thickness was semi-infinite, photons scattered beyond 8 mm were absorbed. Lateral extension of the skin model was infinite. No boundary conditions were applied in lateral directions and no matter how far away a photon exited from its entering position, it was "scored" as a diffusely reflected photon. This makes the model essentially one-dimensional in its light distribution although the photon paths were calculated in three-dimensions. The influence of dermal blood was modeled by averaging optical properties of blood and dermis. To simulate blood in discrete horizontal vessels we used a correction factor [13] to account for a reduced light absorption by the total blood content because blood at the edges of the vessels can shield the photons from reaching the blood in the center. Reflectance was calculated at wavelengths (λ) from 385 nm to 750 nm with increments of 5 nm to cover the visible spectrum [14]. The program simulated isotropic irradiance for all wavelengths considered. Due to the refractive index change (1.0 in air, 1.4 in tissue) a considerable

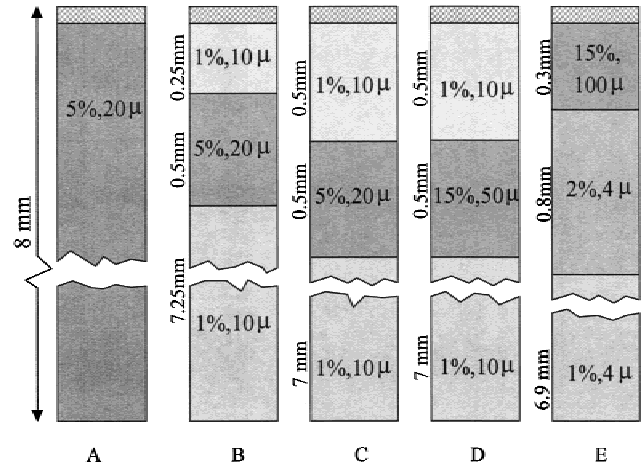


Fig. 1. Five skin models (A-E) used to simulate reflectance spectra after subsequent laser treatments. Thicknesses of dermal layers are indicated alongside the figures whereas dermal blood content and vessel diameter, respectively, are indicated in each of the layers. Each treatment is modeled to result in a reduction of the PWS layer thickness by 0.1 mm. The two-layered model (A) was also used to investigate the influence of skin parameters (dermal blood concentration, vessel diameter, dermal scattering, and epidermal pigmentation) on the color values L^* , a^* , and b^* .

number of photons was specularly reflected. However, we chose to neglect these specularly reflected photons. We used only the diffusely reflected (back scattered) photons, integrating over all exit angles. For blood absorption coefficients, we used an expression for the absorption spectrum of 80% oxygenated blood as given by Svaasand et al. [10]. To investigate influence of blood oxygenation on skin color we proportionally averaged absorption coefficients of hemo- and oxyhemoglobin as given by van Kampen and Zijlstra [15]. The influence of capillary vessels in the papillary dermis was modeled as a homogeneous distribution of 0.4% blood in the epidermis (0.05 mm thickness) [10]. Skin anatomy parameters that were varied are dermal blood concentration (1%, 2%, 5%, and 10%) and PWS vessel diameter (10 μ m, 20 μ m, 50 μ m, and 100 μ m). Svaasand et al. [10] formulated empirical expressions for the dermal scattering coefficient $\mu_{s,der}$ and epidermal absorption coefficient $\mu_{a,epi}$ in which wavelength dependencies are proportional to $(\lambda)^{-1}$ and $(\lambda)^{-4}$, respectively. We adopted their expressions for this study with $\mu_{s,der} = 250 \text{ cm}^{-1}$ or 500 cm^{-1} at 577 nm and the assumption of epidermal scattering to be equal to dermal scattering. Epidermal absorption coefficients were taken as $\mu_{a,epi} = 3, 8, 12, \text{ or } 25 \text{ cm}^{-1}$ at 694 nm for light Caucasian, moderately pigmented, dark pigmented, and African skin [10], respectively. All

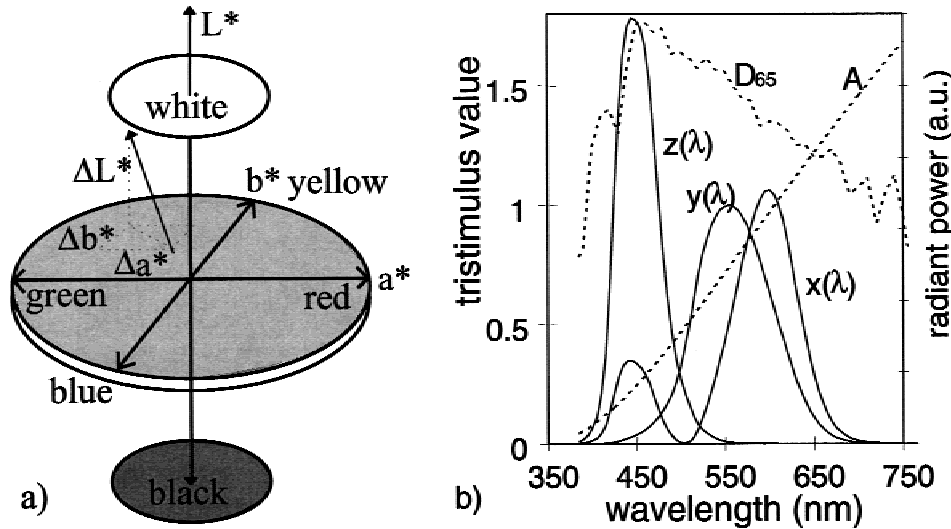


Fig. 2. The CIE 1976 L^* , a^* , b^* color system. **a:** Graphical representation of the CIE 1976 L^* , a^* , b^* color space. Equal distances between two colors approximate equally perceived color differences (arrow). **b:** The tri-stimulus curves $x(\lambda)$, $y(\lambda)$, and $z(\lambda)$ that were used to calculate L^* , a^* , b^* values from the spectra. Radiant powers of CIE standards D_{65} and A are shown, which were used as light sources $S(\lambda)$ to “illuminate” the PWS skin model. Two versions of the tri-stimulus curves have been defined: one set for a “2 degree standard observer”, which we used in this paper and are plotted in b, and one for a “10 degree standard observer” [14].

Differences in perceived color when using the curves for a “10 degree” observer compared to the “2 degree” version are minimal compared to the changes in color as calculated in this article.

the above sets of optical parameters and geometries were used in a two-layered model (epidermis and dermis), i.e., model A in Figure 1.

Simulation of PWS Color Changes After Laser Treatment

Five skin models with two or more layers (Fig. 1) were used to investigate the influence of PWS vessel depth on the perceived color, to simulate color changes in several possible skin geometries after subsequent simulated laser treatments of PWS and to estimate a maximal dermal depth at which blood contributes visibly to the abnormal color of PWS. Model A assumes that the increased dermal blood content of PWS is throughout the entire dermis. The other models assume the PWS to consist of a layer in which dermal blood content is higher (5% or 15%) than normal (1% or 2%). Models A–E are used to compare colors of PWS with PWS layers at different depths, dermal blood concentration, and vessel diameters. Model E is based on histological data from an adult PWS published by Tan et al. [2]. For the first two dermal layers of model E we use the configuration as derived in previous work [6]. After each “treatment,” the upper 0.1 mm of the dermal layer with highest dermal blood concentration (PWS layer) is replaced by normal dermis (dermal blood content 1% and vessel diameter 10 μm for models A to D, and 2% and 4 μm for model E [6]).

Unless mentioned otherwise, epidermal parameters (not indicated in Fig. 1) are $\mu_{a,\text{epi}} = 8$

cm^{-1} at 694 nm and epidermal scattering equals dermal scattering, $m_{s,\text{epi}}$ and $m_{s,\text{der}} = 250 \text{ cm}^{-1}$ at 577 nm for all calculations shown in this article.

Calculation of L^* , a^* , b^* Color Values

Several color systems exist to transform reflectance spectra into color values. We chose a color system recommended by the Commission Internationale de l’Eclairage (CIE) to calculate color and color differences: the CIE (1976) L^* , a^* , b^* system. This system was previously used [16] to calculate color differences in a PWS model as well as clinically to objectively assess color changes after PWS laser treatment. It transforms a reflectance spectrum $R(\lambda)$ into three values, L^* , a^* , and b^* . Each reflection spectrum can be represented by a set of these values, which defines a point in a three-dimensional color space (Fig. 2a). Parameter L^* represents the “lightness” of the spectrum and varies from 0 for a perfect black object to 100 for a total white reflector. Parameter a^* indicates green (negative values) and red (positive values). Similarly, b^* indicates yellow (positive values) and blue (negative values). If both a^* and b^* are very small, the color varies for decreasing values of L^* between 100 and 0 from white to gray to black. Values of a^* and b^* reported in this article are always positive because skin color is yellowish and reddish rather than greenish and bluish. The L^* , a^* , b^* color system defines an approximately uniform color space. This means that color differences, calculated between two colors, are approximately linear with the perceived color difference

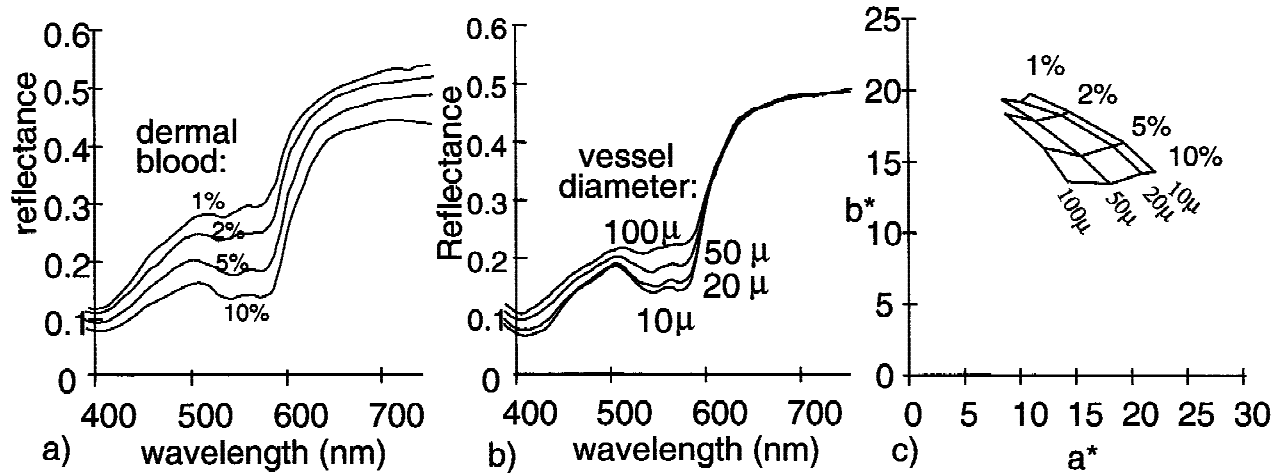


Fig. 3. The influence of dermal blood concentration at constant vessel diameter 50 μm (a) and vessel diameter at constant dermal blood concentration of 5% (b) calculated in the two-layered model. Dermal scattering coefficient is 250 cm^{-1} at 577 nm and epidermal pigmentation is 8 cm^{-1} at 694 nm. Corresponding color values of the spectra in a and b plus combinations of other dermal blood concentrations and vessel diameters are shown in c.

in all parts of the color space. A color difference ΔE (begin and end points of the arrow in Fig. 2a) is defined as $\Delta E = [(\Delta L^*)^2 + (\Delta a^*)^2 + (\Delta b^*)^2]^{1/2}$. The L^*, a^*, b^* system is based on three curves: the tri-stimulus values $x(\lambda)$, $y(\lambda)$, and $z(\lambda)$ [13]. The tri-stimulus values are multiplied by the value of the reflectance spectrum $R(\lambda)$ for each wavelength after which the integral over λ is taken to obtain color values (appendix A, where integration is approximated by summation). Reflectance spectra given in this article always refer to a spectral uniform radiant light source. In practice, the light source is usually not uniform. To calculate color values from the spectra, we considered two standard light sources $S(\lambda)$ defined by CIE: D_{65} and A (Fig. 2b). D_{65} is recommended by CIE to simulate a phase of day light [13]. Light source A is recommended to simulate a regular filament lamp, radiating much more light in the red. However, it is important at this point to realize that we include the color values for both light sources merely as an illustration of the influence of spectral content of light sources on color. In reality, factors such as cloudiness, angle of the sun above the horizon, and air pollution will influence the spectral content as well as the angular distribution of outside illumination conditions. Inside illumination conditions of skin with a filament lamp may be simply altered by changing the color of the wall. Unless mentioned otherwise, all color results in this study are calculated with light source D_{65} .

RESULTS

Influence of Skin Parameters on Reflectance Spectra and Color Values L^* , a^* , b^*

Figure 3a shows reflectance spectra for dermis with dermal blood concentrations 1%, 2%, 5%, and 10%, calculated with a two-layered skin model (model A). An increased dermal blood concentration decreases reflectance throughout the visible spectrum. This effect is stronger at the absorption peaks of oxyhemoglobin (at 415 nm, 544 nm, and 577 nm). Figure 3b shows reflection spectra from a PWS skin model for a constant dermal blood concentration of 5% in vessel diameters of 10 μm , 20 μm , 50 μm , and 100 μm . When distributing the same amount of blood in few large vessels instead of in a larger number of small vessels, reflectance increases mainly in the yellow and blue regions of the spectrum (500 to 580 nm and 400 to 450 nm respectively). In the red part reflectance is independent of vessel diameter. In the yellow and blue wavelength regions penetration depth of light in the blood vessel is much smaller than the vessel diameter. As a result, red blood cells in the center of the vessels are shielded from light by the red blood cells at the edges of the vessels and therefore contribute less to light absorption [14]. This effect is stronger for larger vessels, which explains the higher reflectance levels in those cases. At wavelengths longer than 580 nm light absorption by blood is much lower and the above described effect is negligible. This results in reflectance levels indepen-

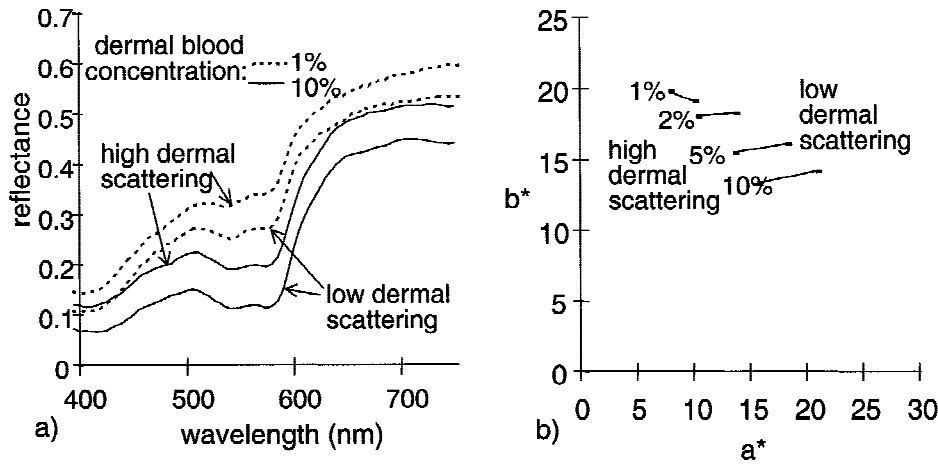


Fig. 4. Influence of dermal scattering on reflectance spectra and perceived color. **a:** Spectra for low and high dermal scattering (250 and 500 cm^{-1} at 577 nm respectively) are given for dermal blood concentrations 1% and 10%. Vessel diameter is 20 μm . All results are from the two-layered model. **b:** Corresponding color values plus the results for dermal blood concentrations 2% and 5%. Dermal scattering has negligible influence on yellowness but a significant influence on redness, especially for large dermal blood concentration.

dent of the vessel diameter. In Figure 3c we show the corresponding color values a^* and b^* of the spectra in Figures 3a and 3b plus color values for other combinations of the dermal blood concentration and vessel diameter used. Figure 3c shows that vessel diameter, varying between 10 and 100 μm , has the same impact on redness (a^*) as dermal blood concentration varying between 10 and 1%. This is because a^* values represent the balance between red and green reflectance levels. Increasing dermal blood concentration yields decreasing reflectance levels over the entire visible spectrum whereas varying vessel diameter has no impact on the red reflectance level albeit a strong influence on the green-yellow levels (Figs. 3a,b). Therefore, even if the reflectance in the green part of the spectrum in Figure 3b varies to a smaller degree than in Figure 3a, the impact of vessel diameter on perceived redness is substantial. We conclude that a PWS with a great number of relatively small vessels appears redder than a PWS with a small number of larger vessels and the same dermal blood content. Furthermore, an increased dermal blood concentration decreases the values of b^* . Values of L^* decrease with increasing dermal blood concentration but increase with increasing vessel diameter. For example, L^* decreases from 60.9 to 46.0 for a 1% to 10% increased dermal blood concentration and 10 μm vessel diameter. Increasing vessel diameter from 10 μm to 100 μm at 5% dermal blood concentration corresponds with an increase of L^* from 51.1 to 56.6.

Figure 4a shows that when doubling dermal scattering coefficient from 250 to 500 cm^{-1} at 577 nm in the two-layered model (A), the relative increase in the green reflectance level is considerably stronger than that in the red reflectance

level for both dermal blood concentrations shown. Therefore, since a^* expresses the balance between red and green, a decrease in redness follows (Fig. 4b). Also, green reflectance increases stronger for 10% than for 1% dermal blood concentrations. This explains that the influence of dermal scattering on the redness (Fig. 4b) is stronger for 10% than for 1% dermal blood concentrations. For both dermal blood concentrations, the decrease in reflectance in the yellow region is comparable to the decrease in the blue part, which means that no significant changes in the value of b^* can be expected. Values of L^* , however, increase significantly when doubling the dermal scattering coefficient. For example, for 1% dermal blood concentration L^* increases from 61.5 to 66.4 and for 10% from 46.9 to 55.8.

Figure 5a shows spectra in which pigmentation was varied whereas other parameters remained constant. Figure 5b shows the corresponding a^* , b^* color values with values of L^* indicated. Although redness is virtually not influenced, yellowness increases with increasing pigmentation while lightness decreases.

To investigate the influence of oxygenation we varied the degree of blood oxygenation in skin with 5% dermal blood concentration and 50 μm vessel diameter. Conversion of the reflectance spectra (not shown) resulted in an increasing redness for increasing oxygenation, mainly due to an increased reflectance at wavelengths larger than 580 nm. For 60%, 80%, and 100% oxygenation, values of a^* are 10.1, 11.2, and 12.8. Corresponding values of L^* are 62.3, 62.0, 61.7, and of b^* 17.6, 17.0, and 16.3, respectively.

Color values calculated with standard illuminant A instead of D_{65} have a large influence on the perceived color, in particular redness. For ex-

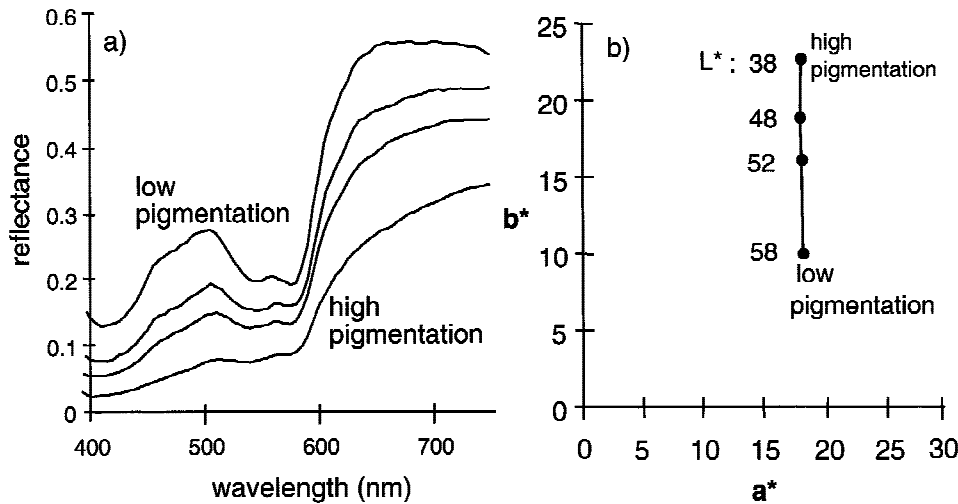


Fig. 5. Influence of epidermal pigmentation on reflectance spectra and perceived color. **a**: Four spectra from the two-layered model in which epidermal pigmentation was varied with constant dermal blood concentration and vessel diameter at 5% and 20 μm respectively. From low to high pigmentation values of $\mu_{a,\text{epi}}$ are 3 cm^{-1} , 8 cm^{-1} , 12 cm^{-1} , and 25 cm^{-1} at 694 nm. Corresponding color values are shown in **b**. Epidermal pigmentation has negligible influence on redness but has large influence on yellowness and lightness.

ample, the curves of Figure 3 give values of a^* that are approximately 7 higher than calculated with D_{65} as shown in Figure 3c. L^* and b^* increase by 2.1 and 2.6, respectively.

Perceived Color Following Simulation of Laser Treatment

Color trajectories after simulated laser "treatments" are shown in Figure 6a for skin models A–E. Figure 6b shows reflectance spectra from skin model E in Figure 1 derived from a histologic picture by Tan et al. [2]. The first "treatment," where the upper 0.1 mm layer of 15% dermal blood in 100 μm diameter vessels is replaced by 2% dermal blood in 4 μm diameter vessels, results in a higher level of reflectance for all wavelengths shown, except for wavelengths from 400 nm to 430 nm (Fig. 6b) where, despite a reduction of dermal blood concentration, level of reflectance decreased. Due to shielding of light by red blood cells at the periphery of vessels (see Materials and Methods), total absorption of light is larger in many small vessels than in fewer large vessels, even though dermal blood concentration is decreased in this example from 15% to 2%. For longer wavelengths, the first "treatment" results in an increase in reflectance of about 1.5% in the red part and approximately 3% in the yellow and green parts of the spectrum. The second "treatment" results in an increase of about 1.5% in the yellow, green, and red parts. The last "treatment" has a very small influence on yellow and green reflectance values, whereas red reflectance still increases. Red light penetrates much deeper (several mm) into the skin tissue and, therefore, reflectance levels are sensitive to changes in blood

concentration and vessel diameters up to skin depths of several millimeters. Yellow and green light penetrate only to relatively shallow depths which explains that the deeper the changes in blood concentration occur, the less the reflectance levels at these wavelengths are affected. This explains that the predicted decrease in redness after the third "treatment" is much smaller than after the first "treatment."

Figure 6a shows that an even more pronounced effect occurs in skin model D. All "treatments" result in a larger value of a^* . The redness increases because replacing a 15% dermal blood concentration by 2% for depths greater than 0.5 mm increases red reflectance but hardly the green reflectance. Comparing color values from the models C and D, in which the PWS layer is at depths 0.25 to 0.75 mm and 0.5 to 1 mm, respectively, we see that the deeper PWS (model C) is less red and less yellow than the shallower PWS (model B). Also, in both cases, changes in a^* and b^* are relatively small following each "treatment." This means that an increased dermal blood concentration at depths larger than 0.5 mm contributes to an abnormal skin color only to a very small degree. Values of L^* for the "untreated" skin models A to E are 52, 58.0, 59.8, 58.9, and 49.8, respectively. These values are increased to 60.9 for models A to D and 56.7 for model E when the entire PWS layer has been "treated." We now define normal skin as the case in which the layer with 5% (models A–C) and 15% (models D and E) is replaced by dermis with lower dermal blood concentration (1% for models A to D, 2% for E). Color differences ΔE between PWS and normal skin are plotted as a function of dermal depth

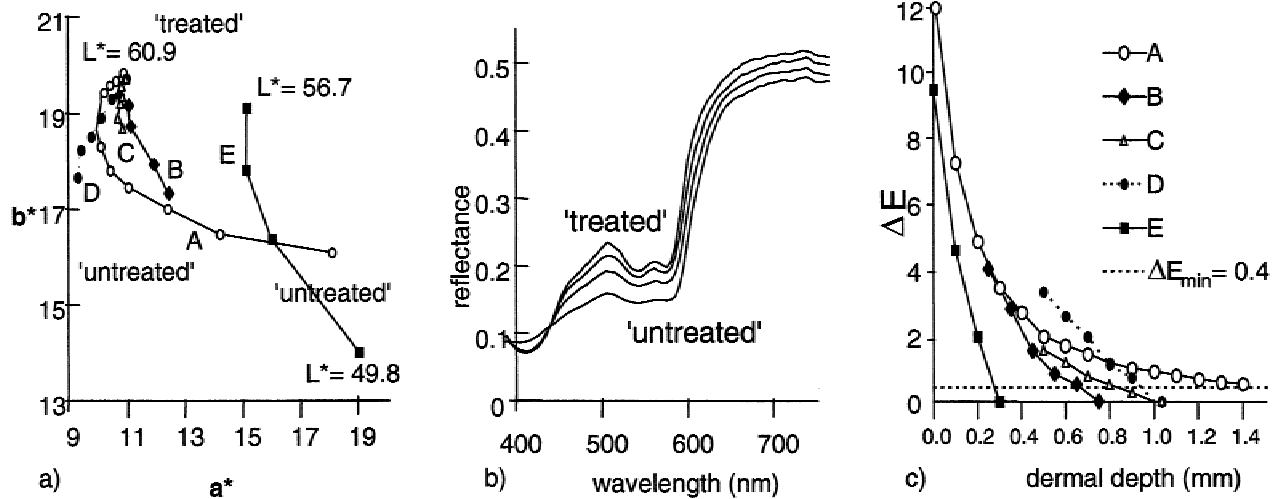


Fig. 6. Color values, reflectance spectra and color differences after simulated "treatments." **a**: Color trajectories in the a^* , b^* plane that correspond to simulation of laser treatment of the PWS defined in Figure 1. For reasons of clarity, color values for model A corresponding to dermal depths larger than 0.5 mm are shown in increments of 0.5 mm rather than 0.1 mm. Values of L^* for the models when completely "treated" are also indicated. The lowest curve in **b** represents calculated reflectance from modeling skin anatomy E (Fig. 1) from Tan et al., 1990 [2]. The upper curves represent spectra as calculated if a 0.1 mm, 0.2 mm, and 0.3 mm thick layer of 15% dermal blood content and 100 μ m vessel diameter of skin anatomy E is replaced by a dermis with 2% dermal blood and 4 μ m vessel diameter. In **c**, color difference values ΔE between untreated PWS models and normal skin decreases with each treatment and consequently a larger dermal depth at which the PWS layer starts. The dashed horizontal line indicates the minimal perceivable color difference assuming $\Delta E_{\min} = 0.4$.

(Fig. 6c). Assuming that the minimal perceivable color difference ΔE_{\min} equals 0.4 [16], indicated by the dashed horizontal line in this figure, we can estimate the maximal dermal treatment depth of the PWS where color difference with the normal skin is less than ΔE_{\min} . For models A–E this is 1.8 mm, 0.65 mm, 0.85 mm, 0.95 mm, and 0.27 mm, respectively.

DISCUSSION

We realize that our calculations and predictions of color include numerous choices, assumptions, and simplifications. Therefore, we would like to stress that the color values as presented here may not necessarily represent true skin color values. We would like to mention some of our assumptions and their possible implications for calculation of skin colors. We assumed epidermal scattering to be equal to dermal scattering, a reasonable assumption in view of the uncertainty in these parameters, and we modeled only one laterally constant epidermal thickness. Since the epidermis is the most superficial layer of the skin (besides the stratum corneum) its influence on reflectance levels is of relatively large importance compared to deeper layers where less light penetrates. Future studies may focus more on mod-

eling the epidermis in more detail rather than the dermal blood layers as in this study. We neglected specularly reflected photons. If included, these photons would have reduced the saturation of the colors because they hardly show spectral dependence. Inclusion of specular reflection also would influence the "glossiness" of objects, which is an aspect of color perception not included in the color system used. A second limitation is that we did not consider angular dependency of the spectral contents of both incident and exiting light. In our approach we integrated all diffusely reflected light whereas in reality the solid angle through which a PWS is observed is considerably smaller than 2π steradians. Considering angular dependencies of the incident and diffusely reflected spectral contents in combination with viewing angles and a realistic solid angle of the eye may show that the colors calculated may vary considerably with viewing angle and illumination conditions.

However, fully appreciating the limitations of this study, we think we have shown that not only dermal blood concentration is an important parameter determining the perceived color in PWS but vessel diameter as well. PWS consisting of many small vessels appear redder than PWS consisting of fewer large vessels, at equal dermal

blood concentration. This means that decreasing the size of vessels alone may not always be sufficient to return PWS skin color to normal. Damaging an ectatic vessel (with an argon laser) may result in formation of two or more smaller vessels [17]. Dermal blood concentration is reduced in this case, which increases the reflectance in the red region of the spectrum. However, several small vessels, close to each other may behave optically as one large vessel, absorbing light of yellow and blue wavelengths equally effectively. For example, if one large vessel of 100 μm is damaged during treatment and two smaller 20 μm diameter vessels are formed during the healing process, lightness and redness may have been decreased to a small degree only. This could explain why some PWS hardly show reduction in both redness and lightness following treatment.

It is difficult to compare our values of maximal depth at which blood contributes visibly to a color difference between normal and PWS skin with those estimated previously by Lakmaker et al. [16]. The number of differences between our approach and theirs are many. For example, we calculated color values from spectra with much smaller wavelength increments, used different sets of skin optical properties and defined anatomical parameters for normal skin differently (1%, 2% dermal blood concentration instead of 0%). Improvements to their approach may be that we corrected for the effect of blood being distributed in vessels rather than assuming it to be distributed homogeneously, and that we used a Monte Carlo algorithm instead of the diffusion approximation to describe photon propagation. Fitting the curve of ΔE as a function of dermal depth (Fig. 6c) with a single exponential function as was done by Lakmaker et al. was not possible for model A. The relative decrease of ΔE for dermal depths smaller than approximately 0.5 mm is well comparable, but beyond this depth it is significantly less strong. This is mainly due to the slight but significant increase in the value of a^* for treatments of PWS layers deeper than approximately 0.6 mm (Fig. 6, models A and D). However, adopting model A as a suitable model and $\Delta E_{\min} = 0.4$ as the minimal perceivable color difference, we confirm the conclusion of Lakmaker et al. that the maximal depth at which blood contributes to an abnormal skin color is larger than 0.9 mm. We stress that a cosmetically acceptable color difference is probably larger than $\Delta E_{\min} = 0.4$, depend-

ing on the homogeneity of the color of normal skin.

The predicted increase in redness, replacing PWS layers by normal skin at dermal depths larger than approximately 0.5 mm is most likely unrealistic following PWS laser treatment. For this phenomenon to occur, replacement of PWS layers at depths larger than the penetration depths of yellow and green light is required. Our purpose was to emphasize that PWS skin color has a complex relationship with skin anatomy and optical properties so that reduction of dermal blood content does not invariably imply a decrease in redness.

REFERENCES

1. Anderson RR, Parrish JA. Microvasculature can be selectively damaged using dye lasers: a basic theory and experimental evidence in human skin. *Lasers Surg Med* 1981;1:263–276.
2. Tan OT, Morrison P, Kurban AK. 585nm for the treatment of port-wine stains. *Plast Reconstr Surg* 1990;86:1112–1117.
3. Smithies DJ, Butler PH. Modeling the distribution of laser light in port-wine stains with the Monte Carlo method. *Phys Med Biol* 1995;40:701–33.
4. Lucassen GW, Verkruysse W, Keijzer M, van Gemert MJC. Light distributions in a port wine stain skin model containing multiple cylindrical and curved blood vessels. *Lasers Surg Med* 1996;18:345–357.
5. Svaasand LO, Fiskerstrand EJ, Kopstadt G, Norvang LT, Svaasand EK, Nelson SJ, Berns MW. Therapeutic response during pulsed laser treatment of port-wine stains: dependence on vessel diameter and depth in dermis. *Lasers Med Sci* 1995;10:235–243.
6. van Gemert MJC, Smithies DJ, Verkruysse W, Milner TE, Nelson SJ. Wavelengths for port wine stain laser treatment: influence of vessel radius and skin anatomy. *Phys Med Biol* 1997;42:41–50.
7. Tang SV, Gilchrist BA, Noe JM, Arndt KA, Bourgelais DB, Itzkan I. In vivo spectrophotometric evaluation of normal, lesional and laser-treated skin in patients with port-wine stains. *J Invest Dermatol* 1983;80:420–423.
8. Bjerring P, Andersen PH. Skin reflectance spectrophotometry. *Photo-Dermatology* 1987;4:167–171.
9. Malm M, Tonnquist G. Telespectrophotometric reflectance measurements for evaluating results after argon laser treatment of port-wine stain compared with natural color system notations. *Ann Plastic Surg* 1988;20:403–409.
10. Svaasand LO, Norvang LT, Fiskerstrand EJ, Stopps EKS, Berns MW, Nelson JS. Tissue parameters determining the visual appearance of normal skin and port-wine stains. *Lasers Med Sci* 1995;10:55–65.
11. van der Horst CMAM, Koster PHL, de Borgie CAJM, Bossuyt PMM, van Gemert MJC. Effect of the timing of treatment of port-wine stains with the flash-lamp-pumped pulsed-dye laser. *N Engl J Med* 1998;338:1028–1033.

12. Keijzer M, Jacques SL, Prahl SA, Welch AJ. Light distributions in artery tissue: Monte Carlo simulations for finite-diameter laser beams. *Lasers Surg Med* 1989;9:148–154.
13. Verkruijsse W, Lucassen GW, de Boer JF, Smithies DJ, Nelson SJ, van Gemert MJC. Modeling light distributions of homogeneous versus discrete absorbers in light irradiated turbid media. *Phys Med Biol* 1997;42: 51–65.
14. Wyszecki G, Stiles WS. Color science: concepts and methods, quantitative data and formulae. New York: John Wiley & Sons; 1982.
15. van Kampen EJ, Zijlstra WG Determination of hemoglobin and its derivatives. In: Sobotka H, Stewart CP, eds. *Advances in clinical chemistry*. New York: Academic Press; 1965. p 158–187.
16. Lakmaker O, Pickering JW, van Gemert MJC. Modeling the color perception of port wine stains and its relation to the depth of laser coagulated blood vessels. *Lasers Surg Med* 1993;13:219–226.
17. Finley JL, Barsky SH, Geer DE, Kamat BR, Noe JM, Rosen S. Healing of port-wine stains after argon laser therapy. *Arch Dermatol* 1981;117:486–489.

APPENDIX A

First, using the diffuse reflectance spectrum $R(\lambda)$, illumination spectrum $S(\lambda)$, and the tri-

stimulus curves $x(\lambda)$, $y(\lambda)$, and $z(\lambda)$ [13], the following parameters are calculated:

$$\begin{aligned}
 k &= \frac{100}{\sum_{385nm}^{780nm} S(\lambda)y(\lambda)\Delta\lambda}, \\
 X &= k \sum_{385nm}^{780nm} R(\lambda)S(\lambda)x(\lambda)\Delta\lambda, \\
 Y &= k \sum_{385nm}^{780nm} R(\lambda)S(\lambda)y(\lambda)\Delta\lambda, \\
 Z &= k \sum_{385nm}^{780nm} R(\lambda)S(\lambda)z(\lambda)\Delta\lambda, \\
 X_n &= k \sum_{385nm}^{780nm} S(\lambda)x(\lambda)\Delta\lambda, \\
 Y_n &= k \sum_{385nm}^{780nm} S(\lambda)y(\lambda)\Delta\lambda, \\
 Z_n &= k \sum_{385nm}^{780nm} S(\lambda)z(\lambda)\Delta\lambda,
 \end{aligned}$$

Then L^* , a^* and b^* are defined as:

$$\begin{aligned}
 L^* &= 116 \left(\frac{Y}{Y_n} \right)^{1/3} - 16 \\
 a^* &= 500 \left[\left(\frac{X}{X_n} \right)^{1/3} - \left(\frac{Y}{Y_n} \right)^{1/3} \right] \\
 b^* &= 200 \left[\left(\frac{Y}{Y_n} \right)^{1/3} - \left(\frac{Z}{Z_n} \right)^{1/3} \right]
 \end{aligned}$$